LA-UR- 01-4442

Approved for public release; distribution is unlimited.

Title:	SPINNING MACROMOLECULAR NANOASSEMBLIES
Author(s):	Peter A. Chiarelli, B-4, Pomona College Joanna L. Casson, C-PCS Daniel J. Holmes - C-PCS, New College of Florida Jeanne M. Robinson-C-PCS Malkiat S. Johal - New College of Florida Hsing-Lin Wang-B-4
Submitted to:	Langmuir

Los Alamos
NATIONAL LABORATORY

Spinning Macromolecular Nanoassemblies

Peter A. Chiarelli,[1,2] Joanna L. Casson,[3] Daniel J. Holmes,[4] Jeanne M. Robinson,[3] Malkiat S. Johal,[4*] Hsing-Lin Wang[2*]

[1]Department of Chemistry, Pomona College, Claremont, CA 91711, USA
2Biosciences Division, Los Alamos National Laboratory, MS J586, Los Alamos, NM 87545, USA
[3]Chemistry Division, Los Alamos National Laboratory, Los Alamos, NM 87545, USA
[4]Division of Natural Sciences, New College of Florida, 5700 N. Tamiami Trail, Sarasota, FL 34243, USA

Abstract

Polyelectrolyte thin films comprised of alternating layers were spin-assembled by sequentially dropping 1mL of cationic and anionic aqueous solutions onto a spinning substrate. In this work, we show the applicability of our technique to multiple systems, and present two methods for producing linear film growth. The polycations used were PEI (poly(ethylenimine), PDDA (poly(diallyldimethyl ammonium chloride), PAH (poly(allylamine hydrochloride), and two poly(propylenimine) dendrimers (generations 3.0 and 4.0). The polyanions used were PAZO (poly[1-[4-(3-carboxy-4-hydroxy-phenylazo)benzene sulfonamido]-1,2-ethanediyl, sodium salt]), PSS (poly(styrenesulfonate)), and PAA (poly(acrylic acid)). Five polyanion/polycation combinations were chosen and spin-assembled at a speed of 3000 RPM. Layer thicknesses for all systems were determined using single-wavelength ellipsometry. UV-vis spectroscopy was also used to measure deposition amounts in films incorporating the chromophoric polyanions PAZO and PSS. Films incorporating gen 3.0 dendrimer and PAZO showed more interpenetration between layers than films assembled from gen 4.0 dendrimer and PAZO. We also demonstrate the ability to spin-assemble multi-layered thin films up to 50 bilayers with linear increases in deposition amount between bilayers.

* To whom correspondence should be addressed. MSJ: Phone: (941) 359-4450; Email: johal@sar.usf.edu; HSW: Phone: (505) 667-9944; Email: hwang@lanl.gov

Introduction

Spin coating, a technique used for casting chemical layers onto a rotating substrate, has been used extensively to prepare thin films for diverse industrial applications such as photolithography,[1] light emission,[2,3] nuclear track detection,[4] and gas sensing[5,6]. While the practice of spin coating has existed since the 1920s,[7] mathematical modeling of the spin-coating process began in the late 1950s when Emslie et al. described the radial flow of liquids deposited on rotating substrates.[8] Since then, monolayer film formation dynamics has been studied both experimentally and theoretically. Effects of solvent evaporation,[9,10,11] liquid viscosity,[12,13] spin speed,[14,15] spin time,[16,17] solute concentration,[18,19] and solute molecular weight[20] have been examined for a variety of spin-coated systems. The simplicity, time efficiency, and inexpensiveness of spin coating make it a practical method for the deposition of thin polymer films. *Spin-assembly* is a specialized application of spin-coating, in which polyelectrolyte multi-layers are self-assembled onto spinning substrates. This process utilizes electrostatic forces to facilitate the deposition process.

Currently, ultrathin organic films of alternating charged layers are constructed by ionic self-assembly,[21,22,23,24,25] vapor deposition,[26,27] and Langmuir-Blodgett deposition[28,29] for use in applications[30,31,32,33,34] such as biological sensing, optical switching, and waveguiding. Using electrostatic forces to spontaneously induce desired molecular architectures in layer-by-layer organic films has opened up new applications in nonlinear optics for such devices.[35,36,37] For example, the ability to modulate a second harmonic signal through the deposition of alternating layers has recently been shown by

Casson et al.[38] In multi-layered films, the effects of the substrate,[39] solution pH,[40] deposition temperature,[41] and salt concentration[42,43] have been explored extensively.

New mechanisms of film formation, such as spin-assembly, can play a significant role in the rapidly expanding field of thin film formation. The spin-assembly of polyelectrolyte multi-layer systems has recently been described for 10 bilayers of the polyelectrolytes PEI and PAZO.[44] Spin-assembly, the alternating deposition of dilute ($\sim 10^{-3}$ M) polyelectrolyte solutions onto a spinning substrate, is a novel method for constructing self-assembled thin films with monolayer thicknesses on the order of Angstroms. Instead of establishing a thermodynamic equilibrium as in ionic self-assembly, spin-assembly takes advantage of short liquid-substrate contact times and variable spin speeds to quickly deposit controlled amounts of material onto a film surface.[45] As in spin-casting, the films are formed without reaching a thermodynamic deposition equilibrium.[46] Multi-layer thickness can be controlled through the manipulation of polymer concentration and/or spin speed.[47]

In this work, we demonstrate the application of spin-assembly to a variety of polyelectrolytes, including both polymers and dendrimers. The polycations used were PEI (poly(ethylenimine), PDDA (poly(diallyldimethyl ammonium chloride), PAH (poly(allylamine hydrochloride), and two poly(propylenimine) dendrimers (generations 3.0 and 4.0). The polyanions used were PAZO (poly[1-[4-(3-carboxy-4-hydroxy-phenylazo)benzene sulfonamido]-1,2-ethanediyl, sodium salt]), PSS (poly(styrenesulfonate)), and PAA (poly(acrylic acid)) (Figure 1). From these polyelectrolytes, we chose to spin-assemble thin films of PEI/PAZO, generation 3.0 dendrimer/PAZO, generation 4.0 dendrimer/PAZO, PSS/PAH, PDDA/PAA, and repeat

monolayers of a single charged material. We show that spin-assembly can be used successfully even in conditions where electrostatics does not play a primary role. Additionally, we have constructed 50 bilayer PEI/PAZO films that show linear growth in the amount of adsorbed material.

Experimental Method

Materials. A variety of polyelectrolyte systems were used in the spin-assembly process. PAZO (poly[1-[4-(3-carboxy-4-hydroxy-phenylazo)benzene sulfonamido]-1,2-ethanediyl, sodium salt]), PSS (poly(styrenesulfonate)), and PAA (poly(acrylic acid)) were the primary polyanions. PEI (poly(ethylenimine), PDDA (poly(diallyldimethyl ammonium chloride), PAH (poly(allylamine hydrochloride)), and two poly(propylenimine) dendrimers (generations 3.0 and 4.0) were the polycations used. All spin-assembled materials were purchased from Aldrich and prepared by dilution in Millipore water (resistance >18.0 MΩ) at concentrations of 1 and 10 mM (calculated using monomeric weights).

Substrate Preparation. Substrates for film deposition were glass microscope slides, round 1 inch polished silicon wafers, and round 1 inch quartz crytal plates. Substrates were prepared by immersion in a 30:70 H_2O_2/H_2SO_4 mixture for one hour at 80° C (pirhana etch treatment). Following this treatment, substrates were rinsed thoroughly with pure water, sonicated for 15 min to remove any remaining etch solution, and stored in water. Immediately prior to film deposition, bare substrates were spun at 3000 RPM, and then heated (110° C) or subjected to a vacuum (381 mm Hg at 40° C) for 1 min to remove the surface water.

Film Construction. Thin films were spin-assembled from aqueous polymer solutions on a Headway Research photoresist spinner at 3000 RPM. The spin-assembly process consisted of pipetting 1 mL of polycation solution onto a spinning substrate and spinning for 1 min. The substrate was then heated at 110° C for 1 min or exposed to a vacuum (381 mm Hg at 40° C) for 1 min, with the exception of the dendrimer/PAZO films , which were heated for three minutes at 110° C. The heat-dried substrates were cooled for 1 min following heating. 1mL of polyanion was then deposited onto the spinning film surface, and spun for 1 min. Vacuum or heat drying and cooling was repeated as before. The deposition of polycation and polyanion layers was repeated until a multi-layered film with the desired number of bilayers was constructed.

Film Characterization. UV-vis measurements of the multi-layered films built on glass and quartz substrates were taken between 300-700 nm on a Perkin-Elmer Lambda 19 spectrophotometer and between 190-700 nm on a Varian Cary 300 spectrophotometer. Spectra were obtained every layer.

Ellipsometric measurements were collected on a Rudolph Research AutoEL III single-wavelength null-ellipsometer. 1" round single-side-polished silicon wafers were used as substrates for films characterized by ellipsometry. Similar silicon oxide surface layers of both substrate types (glass and silicon) provided reproducible surface conditions for film deposition. Data was collected at a beam incidence angle of 70° and a wavelength of 632.8nm. A refractive index of $1.5 + 0i$ was used to manually calculate ellipsometric film thicknesses from Δ and Ψ parameters. Substrate measurements were subtracted from film measurements to determine total ellipsometric film thickness.

Results and Discussion

Consistency of Adsorption. A significant factor contributing to the linear growth of spin-assembled films is the removal of residual water from each solid layer. Since all of our films are assembled from dilute aqueous solution, water could remain trapped on the surface and inside the bulk of our films. Simply blow drying the film surface with N_2 gas, without using heat or vacuum, resulted in irregular film growth. Sometimes, the UV-vis absorbance spectra of deposited chromophoric layers showed no increase over those of previous chromophoric layers. This lack of consistent growth in the UV-vis absorbance suggested that in some deposition cycles no polymer was deposited. As reported previously, oven drying at 110° C prior to every monolayer was key to linear film growth.[48] We have recently found that placing the substrate in a vacuum at 381 mm Hg. after each deposition cycle yields a similar uniformity in the amount of adsorbed material. The above result supports our hypothesis that removal of water is key to successful deposition of multi-layered films. Figure 2 shows the layer thicknesses for PEI/PAZO films built using both oven drying and vacuum suction. The total film thickness after 10 bilayers is approximately equivalent (~100 Å) for both films. However, the films show different behavior upon treatment with either heat or vacuum. After heat treatment, a series of small decreases (~1 Å) are observed in ellipsometric thickness. After vacuum treatment, ellipsometric thickness actually increases by approximately 1 Å. Although the films both display linear increases in ellipsometric thickness after each bilayer, the drops and increases in thickness after drying indicate that there is some difference in film morphology between methods. We are currently investigating this difference using AFM and second harmonic generation.

Diverse Application of Spin-Assembly.

PEI/PAZO. We have already explored the PEI/PAZO system using both UV-vis spectroscopy and ellipsometry[49]. In the current study, a 50 bilayer polyelectrolyte film was constructed from 1 mM solutions of PEI and PAZO at a spin speed of 3000 RPM to show the feasibility of spin-assembly for building large-scale nanoassemblies. The phenylazobenzene conjugated system on PAZO absorbs light in the visible region allowing us to monitor a peak around 364 nm. The peak absorbances of the UV-vis spectra taken aften each bilayer show a linear increase from 1 to 50 bilayers (Figure 3a). Although the λ_{max} of the first PAZO layer occurs at approximately 364 nm, Figure 3b shows a red-shift in λ_{max} as the first 10 bilayers are built. This initial shift in λ_{max} peaks around the 10th bilayer, but slowly blue-shifts back to the original λ_{max} value between bilayers 10 and 40. Bilayers 40-50 show little change in λ_{max}. Similar shifting patterns from red to blue have been reported in ionically-self-assembled PEI/PAZO films.[50] Possible explanations of such shifting patterns include changes in chromophore aggregation as the film grows.

As seen in Figure 3c, the 50 bilayer film shows a minor alteration in growth rate around the 16th bilayer. Although the increases in amount of PAZO are primarily linear, the changes in deposition amount can be best modeled by two separate lines. It is well established that the effect of the negatively charged substrate gradually diminishes as films are built, eventually revealing deposition behavior dominated by the charge density and steric parameters of the polyelectrolytes.[51] Therefore, the change in slope around bilayer 16 can be attributed to the diminishing influence of the substrate on the adsorption of the polymer bilayers.

Dendrimer/PAZO. PAZO was also assembled with two macromolecules, generation 3.0 and generation 4.0 poly(propylenimine) dendrimers. These dendrimers contain many (30-62) protonation sites within a very small (14-21 Å diameter) area.[52] This allows them to serve as strong polycations in the ionic self-assembly process.[53,54] Figures 4a and 4b show consistent film deposition for generation 3.0 dendrimer and PAZO in both ellipsometric and UV-vis measurements for spin-assembled systems. In addition, these figures also show the linearity of films assembled using generation 4.0 dendrimer and PAZO, a system that has not been studied before. Achieving this linear growth in both UV-vis absorbance and thickness required a slight change in our standard procedure. Instead of heating the substrate for one minute at 110° C, it was heated for three minutes. Without the additional heating time, uniform increases in the maximum UV-vis absorbance were not observed. Increased heating is needed for the dendrimer layers due to the multiple hydrogen bonding sites and the resultant tendency to retain water.

As Figure 4a shows, the maximum UV-vis absorbances of films built from the two generations of dendrimers are similar, but Figure 4b illustrates that the ellipsometric thicknesses are much larger for generation 4.0 than generation 3.0 dendrimer. This can be explained by looking at the layer-by-layer ellipsometric data in Figures 5a and 5b. In the generation 3.0/PAZO system, the addition of dendrimer to the system causes either no increase or a decrease in the overall thickness of the film. This probably arises from increased interpenetration of the dendrimer layer with the PAZO layer, thus reducing the overall film thickness. In the generation 4.0 dendrimer/PAZO system, the ellipsometry data shows a continual increase in film thickness as each monolayer is added. We infer

that it is more difficult for the generation 4.0 dendrimer to interpenetrate the PAZO layers because of its increased size. In Figure 5b, only 14 of the 20 layers are shown, due to constraints of the ellipsometric data analysis program. However, the 14th layer of the generation 3.0 is almost twice as thick as the 14th layer for the generation 4.0 dendrimer film.

PAH/PSS. PAH and PSS were also spin-assembled and characterized using UV-vis spectroscopy and ellipsometry. For all PAH/PSS films, quartz crystal substrates were used to monitor the PSS absorption peak around 225 nm. UV-vis spectra (Figure 6a) show that the amount of PSS deposited increases linearly for every bilayer. Ellipsometric measurements (Figure 6b) for each PSS outerlayer also show linear growth in film thickness.

In our other systems characterized by ellipsometry, layers within the first 50-80 Å of the film show a slightly different rate of thickness growth than the remainder of the film. We believe this difference to be one of conformation and packing structure, not deposition amount, since UV-vis measurements on chromophoric polyelectrolytes show no significant deviations within the first few bilayers. This effect has been observed in both dipped and spin-assembled PEI/PAZO films. The PAH/PSS multi-layered film, however, does not show any slope change up to 10 bilayers. Due to the thinness of the film, the diminishing effects of the substrate after 50-80 Å may not be obvious, since the 10 bilayer film is only 90 Å thick. Cho, et. al., have recently reported a different spin-method for the construction of PAH/PSS multi-layer films.[55] They observed linear increases in polymer adsorption, as monitored every fourth bilayer by UV-vis spectroscopy.

PDDA/PAA. Figure 7 shows 18 spin-assembled bilayers of polycationic PDDA and polyanionic PAA characterized by ellipsometry. This system shows a change in thickness growth rate around the 6th bilayer (~80 Å thickness). We speculate that this difference in slope is due to conformational changes much like the PEI/PAZO film and not to changing deposition amounts. Beyond the 6th bilayer layer, we observe linear thickness increases of ~50 Å per bilayer.

Electrostatic Effects. One important advantage of spin assembly is that the film formation process is not solely dependent on electrostatics to induce deposition. For example, we have reported the linear growth of a PAZO layer over 10 deposition cycles on top of a single positively charged PEI underlayer.[56] In this work, we report the ability to build a thick PEI layer on a bare, negatively charged substrate using 10 deposition cycles (Figure 8). With each deposition cycle, we observe linear growth behavior. Similar to the growth behavior of bilayer films, a change in slope is observed in the 50-80 Å region. This change in slope for a pure PEI film demonstrates that the substrate effect is seen in all types of films, not solely films of alternating multi-layers. The thickness increase of the PEI layer after each deposition is comparable to that deposited when the PEI adsorbs onto a PAZO layer. As seen in the bilayer films, a change in slope around 50-80 Å is seen in the PEI thickness data. Additionally, 10 deposition cycles of PAZO on top of a bare substrate displayed linear growth between depositions (Figure 9). Growth of the PAZO film was monitored by both UV-vis spectroscopy and ellipsometry. For PAZO, total amounts deposited and corresponding thicknesses were much lower than for PEI. Weill and Dechenaux state that the spin-coating process relies heavily on polymer chain entanglement to form solid layers.[57] It is likely that interlayer

entanglements contribute to the formation of our PEI/PEI and PAZO/PAZO layer combinations, since electrostatic attraction cannot occur between layers.

The potential applications of such physical layer formation are great, since multi-layer composite films can now be assembled that incorporate multiple non-electrostatically favored layers along with bilayers of alternating charge to induce specific nanoscale ordering within the film not possible through conventional dipping techniques.

Summary

For a variety of systems incorporating both organic polymers and dendrimers, we have demonstrated control over the formation of multi-layered films using spin-assembly. The construction of a 50 bilayer PEI/PAZO film shows that the technique is not limited to the 10 bilayer systems we have used for characterization. Spin-assembly can be used for the fabrication of conventional alternating layer-by-layer assemblies, as well as a new host of non-electrostatically-driven layer assemblies. Using vacuum drying (as well as oven drying) to induce linearity in spin-assembled systems makes the process a more versatile method of easily and inexpensively fabricating macromolecular nanoassemblies.

Acknowledgements

This work was supported by the Laboratory Directed Research and Development program at Los Alamos National Laboratory under the auspices of the United States Department of Energy. PAC acknowledges the Department of Chemistry, Pomona College, for support. MSJ and DJH were also supported by a grant from the Camille and

Henry Dreyfus foundation and New College of Florida. We thank Greg Fisher and Atul Parikh for assistance with ellipsometric measurements.

---

[1] Murarka, S.P.; Peckerar, M.C. *Electronic Materials Science and Technology*; Academic Press: San Diego, CA, 1989; pp 483-494.
[2] Elschner, A.; Bruder, F.; Heuer, H.W.; Jonas, F.; Karbach, A.; Kirchmeyer, S.; Thurm, S.; Wehrmann, R. *Synth. Metals* **2000**, *111-112*, 139.
[3] Shi, Y.; Liu, J.; Yang, Y. *J. Appl. Phys.* **2000**, *87*, 4254.
[4] Nadkarni, V.S.; Samant, S.D. *Rad. Meas.* **1997**, *27*, 505.
[5] Bae, H.Y.; Choi, G.M. *Sensors and Actuators B* **1999**, *55*, 47.
[6] Nicolau, M.; del Rey, B.; Torres, T.; Mingotaud, C.; Delhaes, P.; Cook, M.J.; Thorpe, S.C. *Synth. Met.* **1999**, *102*, 1462.
[7] Walker, P.H.; Thompson, J.G. *Proc. Am. Soc. Test. Mater.* **1922**, *22*, 464.
[8] Emslie, A.G.; Bonner, F.T.; Peck, L.G.; *J. Appl. Phys.* **1958**, *29*, 858.
[9] Lawrence, C.J.; *Phys. Fluids*. **1990**, *2*, 453.
[10] Chen, B.T. *Polym. Eng. Sci.* **1983**, *23*, 399.
[11] Jenekhe, S.A. *Ind. Eng. Chem. Fundam.* **1984**, *23*, 425.
[12] Flack, W.W.; Soong, D.S.; Bell, A.T.; Hess, D.W. *J. Appl. Phys.* **1984**, *56*, 1199.
[13] Borkar, A.V.; Tsamopoulos, J.A.; Gupta, S.A.; Gupta, R.K. *Phys. Fluids* **1994**, *6*, 3539.
[14] Meyerhofer, D. *J. Appl. Phys.* **1978**, *49*, 3993.
[15] Lawrence, C.J.; *Phys. Fluids* **1988**, *31*, 2786.
[16] Gu, J.; Bullwinkel, M.D.; Campbell, G.A. *Polym. Eng. Sci.* **1996**, *36*, 1019.
[17] Ohara, T.; Matsumoto, Y.; Ohashi, H. *Phys. Fluids* **1989**, *1*, 1949.
[18] Ton-That, C.; Shard, A.G.; Bradley, R.H. *Langmuir* **2000**, *16*, 2281
[19] Meyerhofer, D. *J. Appl. Phys.* **1978**, *49*, 3993.
[20] Spangler, L.L.; Torkelson, J.M.; Royal, J.S. *Polym. Eng. Sci.* **1990**, *30*, 644.
[21] Decher, G.; Hong, J.D.; Schmit, J. *Thin Solid Films* **1992**, *210/211*, 831.
[22] Heflin, J.R.; Liu, Y.; Figura, C.; Marciu, D.; Claus, R.O. *Prc. SPIE* **1997**, *3147*, 10.
[23] Shiratori, S.S.; Rubner, M.F. *Macromolecules* **2000**, *33*, 4213.
[24] Mendelsohn, J.D.; Barrett, C.J.; Chan, V.V.; Pal, A.J; Mayes, A.M.; Rubner, M.F. *Langmuir* **2000**, *16*, 5017.
[25] Lvov, Y.; Yamada, S.; Kunitake, T. *Thin Solid Films* **1997**, *300*, 107.
[26] Usui, H. *Thin Solid Films* **2000**, *365*, 22.
[27] Tamada, M.; Koshidawa, H.; Suwa, T.; Yoshioka, T.; Usui, H.; Sato, H. *Polymer* **2000**, *41*, 5661.
[28] Johal, M.S.; Parikh, A.N.; Lee, Y.; Casson, J.L.; Foster, L.; Swanson, B.I.; McBranch, D.W.; Li, D.W.; Robinson, J.M. *Langmuir* **1999**, *15*, 1275.
[29] Ulman, A. *An Introduction to Ultrathin Organic Films from Langmuir-Blodgett to Self-Assembly*, Academic Press, San Diego, CA **1991**.
[30] Kajzar, F.; Swalen, J.D. Eds. *Organic Thin Films for Waveguiding Nonlinear Optics*; Gordon and Breach Publishers: Amsterdam, 1996.

[31] Li, D.W.; Ramos, O., Jr. In *Photonic Polymer Systems*; Wise, D.L., Wnek, G.E., Tantolo, D.J., Cooper, T.M., Gresser, J.D., Eds; Marcel Dekker: New York, 1998.
[32] Modium, D.; Miller, R. Eds. *New Developments in Construction and Function of Organic Thin Films*; Elsevier: Amsterdam, 1996.
[33] Aldrovandi, S.; Borsa, F.; Lascialfari, A.; Tongnetii, V.J *J. Appl. Phys.* **1991**, *6*, 5914.
[34] Li, D.Q.; Marks, T.J.; Zhang, C.; Wang, G.W.; *Synth. Met.* **1991**, *41*, 3157.
[35] Johal, M.S.; Cao, Y.W.; Chai, X.D.; Smilowitz, L.B.; Robinson, J.M.; Li, T.J.; McBranch, D.; Li, D.Q. *Chem. Mater.* **1999**, *11*, 1962.
[36] Samyn, C.; Verbiest, T.; Persoons, A. *Macromol. Rapid Comm.* **2000**, *21*, 1.
[37] Lvov, Y.; Yamada, S.; Kunitake, T. *Thin Solid Films* **1997**, *300*, 107.
[38] Casson, J.L.; McBranch, D.W.; Robinson, J.M.; Wang, H.L.; Roberts, J.B.; Chiarelli, P.A.; Johal, M.S. *J. Phys. Chem. B* **2000**, *104*, 11996.
[39] Phuvanartnuruks, V.; McCarthy, T.J.; M*acromolecules* **1998**, *31*, 1906.
[40] Park, S.Y.; Barrett, C.J.; Rubner, M.F.; Mayes, A.M. *Macromolecules* **2001**, *34*, 3384.
[41] Lvov, Y.; Decher, G. Mohwald, H. *Langmuir*, **1993**, *9*, 481.
[42] Dubas, S.T.; Schlenoff, J.B. *Macromolecules* **1999**, *32*, 8153.
[43] Rojas, O.J.; Claesson, P.M.; Muller, D.; Neuman, R.D. *J. Coll. Int. Sci.* **1998**, *205*, 77.
[44] Chiarelli, P.A.; Johal, M.S.; Casson, J.L.; Roberts, J.B.; Robinson, J.M.; Wang, H.L. *Adv. Mater.* **2001**, *13*, page number .
[45] **Chiarelli, P.A.; Johal, M.S.; Casson, J.L.; Roberts, J.B.; Robinson, J.M.; Wang, H.L. *Adv. Mater.* 2001, *13*, page number.**
[46] Walheim, S.; Boltau, M.; Mlynek, J.; Krausch, G.; Steiner, U. *Macromolecules* **1997**, *30*, 4995.
[47] **Chiarelli, P.A.; Johal, M.S.; Casson, J.L.; Roberts, J.B.; Robinson, J.M.; Wang, H.L. *Adv. Mater.* 2001, *13*, page number.**
[48] **Chiarelli, P.A.; Johal, M.S.; Casson, J.L.; Roberts, J.B.; Robinson, J.M.; Wang, H.L. *Adv. Mater.* 2001, *13*, page number.**
[49] **Chiarelli, P.A.; Johal, M.S.; Casson, J.L.; Roberts, J.B.; Robinson, J.M.; Wang, H.L. *Adv. Mater.* 2001, *13*, page number.**
[50] Dante, S.; Advincula, R.; Frank, C.W.; Stroeve, P. *Langmuir* **1999**, *15*, 193.
[51] Decher, G. *Science*, **1997**, *277*, 1232.
[52] Zeng F.; Zimmerman, S.C. *Chem. Rev.* **1997**, *97*, 1681.
[53] van Duijvenbode, R.C.; Koper, G.J.M.; Böhmer M.R. *Langmuir* **2000**,*16*, 7713.
[54] **Casson, J.L.; McBranch, D.W.; Robinson, J.M.; Wang, H.L.; Roberts, J.B.; Chiarelli, P.A.; Johal, M.S. *J. Phys. Chem. B* 2000, *104*, 11996.**
[55] Cho, J.; Char, K.; Hong, J.D.; Lee, K.B.; *Adv. Mater.* **2001**, *13*, 1076.
[56] **Chiarelli, P.A.; Johal, M.S.; Casson, J.L.; Roberts, J.B.; Robinson, J.M.; Wang, H.L. *Adv. Mater.* 2001, *13*, page number.**
[57] Weill, A.; Dechenaux, E. *Polym. Eng. Sci.* **1988**, *28*, 945.

Figure Captions

Figure 1. Materials used to investigate film formation. Anions were a) PAZO (poly[1-[4-(3-carboxy-4-hydroxyphenylazo)benzenesulfonamido]-1,2-ethanediyl, sodium salt]), b) PAA (poly(acrylic acid)), and c) PSS (poly(styrenesulfonate)). Cations were d) PEI (poly(ethylenimine)), e) PAH (poly(allylamine hydrochloride)), f) PDDA (poly(diallyldimethyl ammonium chloride)), g) generation 3.0 poly(propylenimine) dendrimer, and h) generation 4.0 poly(propylenimine) dendrimer.

Figure 2. Ellipsometric thicknesses taken before and after drying every monolayer of 1mM PEI (■) / 1mM PAZO (●) films spin-assembled at 3000 RPM using a) heat treatment or b) vacuum treatment to dry the films. Measurements taken before heat or vacuum treatment for PEI (○) and PAZO (□) are represented by half (X.5) values. Inset: close-up for monolayers 16 and 17 to show effects of each treatmtent method.

Figure 3. 50 bilayer film of 1mM PEI / 1mM PAZO spin-assembled at 3000 RPM. a) UV-visible spectra (spectrum for every 10^{th} layer is shown in bold). b) Location of λ_{max}. c) Absorbance at λ_{max}.

Figure 4. a) UV-visible absorbance at λ_{max} for films built from 1mM PAZO and either 1mM gen 3.0 (▲) or gen 4.0 (●) dendrimer. b) Ellipsometric thickness at the film center for 1mM PAZO / 1mM gen 3.0 (▲) or gen 4.0 (●) dendrimer films. All films were spin-assembled at 3000 RPM.

Figure 5. Ellipsometric thickness of monolayers built from 1mM PEI (■) and 1mM PAZO (●) in a) gen 3.0 dendrimer and b) gen 4.0 dendrimer films spin-assembled at 3000 RPM

Figure 6. a) UV-visible absorbance at λ_{max} for 10 bilayers of a 1mM PAH / 1mM PSS film spin-assembled at 3000 RPM. b) Ellipsometric thickness for 10 bilayers of PAH / PSS.

Figure 7. Ellipsometric thickness for 18 bilayers of a 1mM PDDA / 1mM PAA film spin-assembled at 3000 RPM.

Figure 8. Ellipsometric Thickness for 10 monolayers of 10mM PEI spin-assembled at 3000 RPM.

Figure 9. a) UV-visible absorbance for 10 monolayers of 1mM PAZO spin-assembled at 3000 RPM. b) Ellipsometric thickness for 10 monolayers of 1mM PAZO.

Figure 1

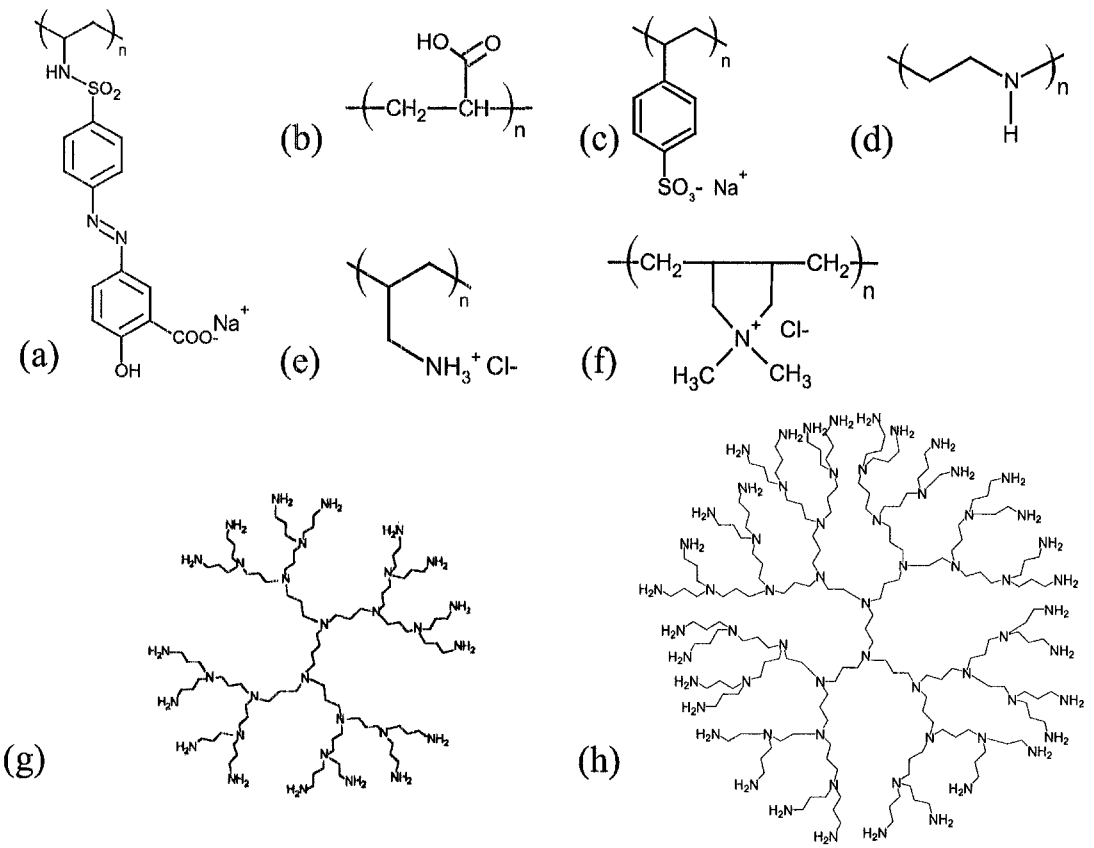

Figure 2

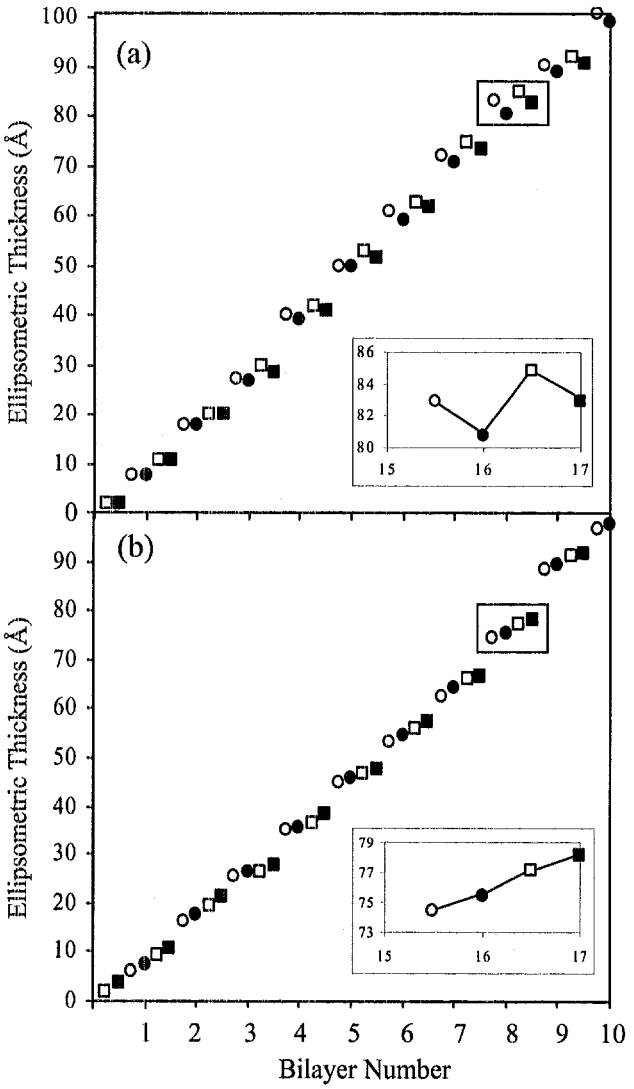
(a)
(b)
Ellipsometric Thickness (Å)
Ellipsometric Thickness (Å)
Bilayer Number
0
10
20
30
40
50
60
70
80
90
100
1
2
3
4
5
6
7
8
9
10
80
82
84
86
73
75
77
79
15
16
17

Figure 3

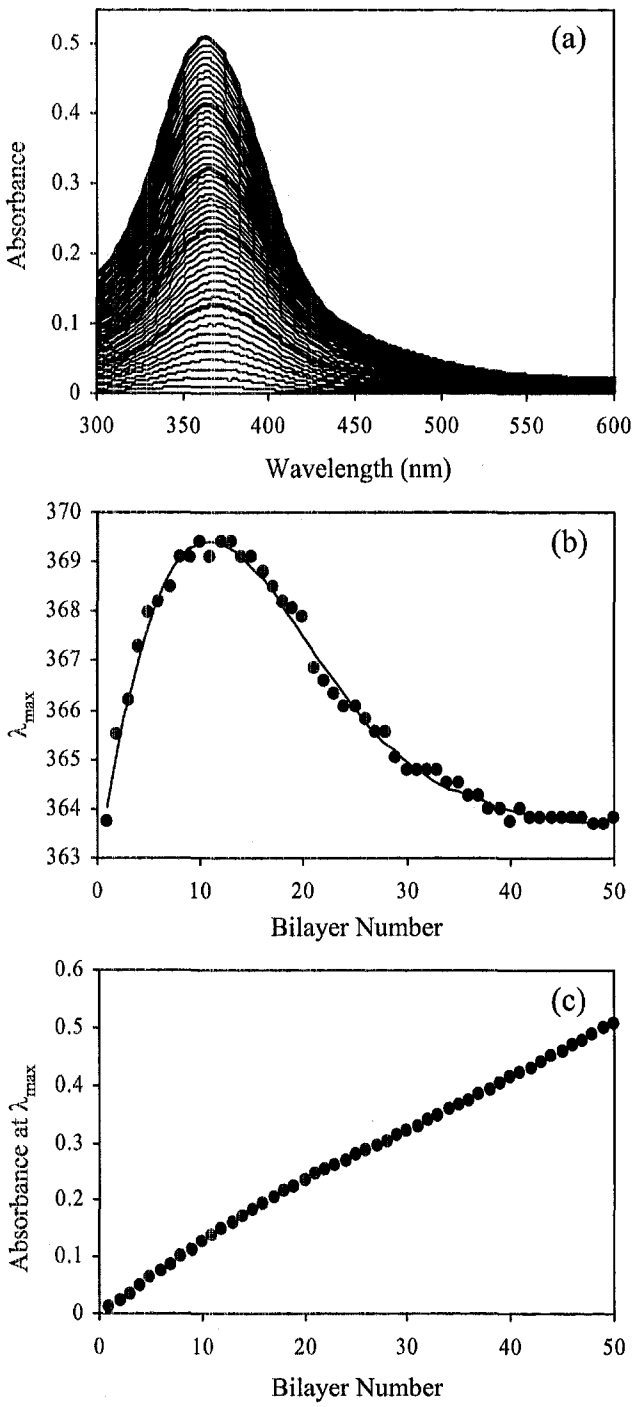
(a)
Absorbance
0.5
0.4
0.3
0.2
0.1
0
300
350
400
450
500
550
600
Wavelength (nm)
(b)
λ_{max}
370
369
368
367
366
365
364
363
0
10
20
30
40
50
Bilayer Number
(c)
Absorbance at λ_{max}
0.6
0.5
0.4
0.3
0.2
0.1
0
0
10
20
30
40
50
Bilayer Number

Figure 4

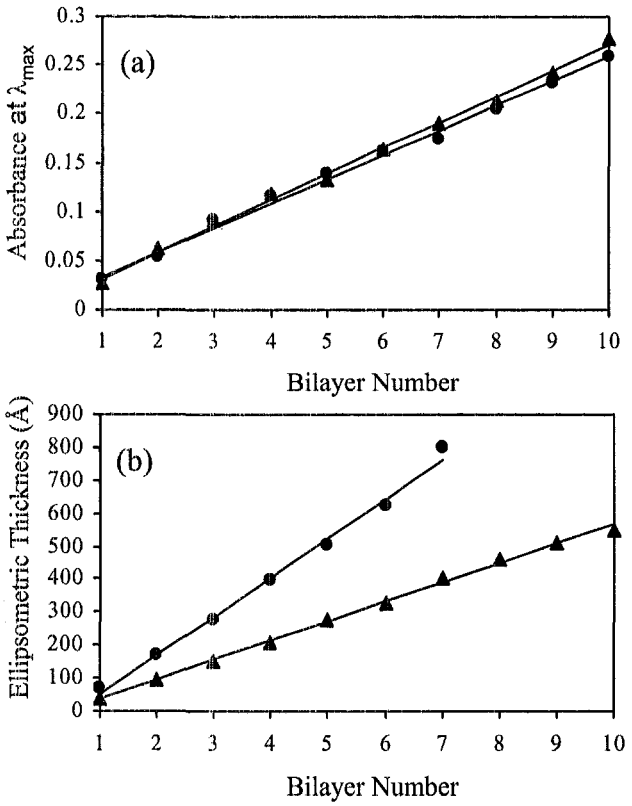
(a)
Absorbance at λ_{max}
0.3
0.25
0.2
0.15
0.1
0.05
0
1 2 3 4 5 6 7 8 9 10
Bilayer Number
(b)
Ellipsometric Thickness (Å)
900
800
700
600
500
400
300
200
100
0
1 2 3 4 5 6 7 8 9 10
Bilayer Number

Figure 5

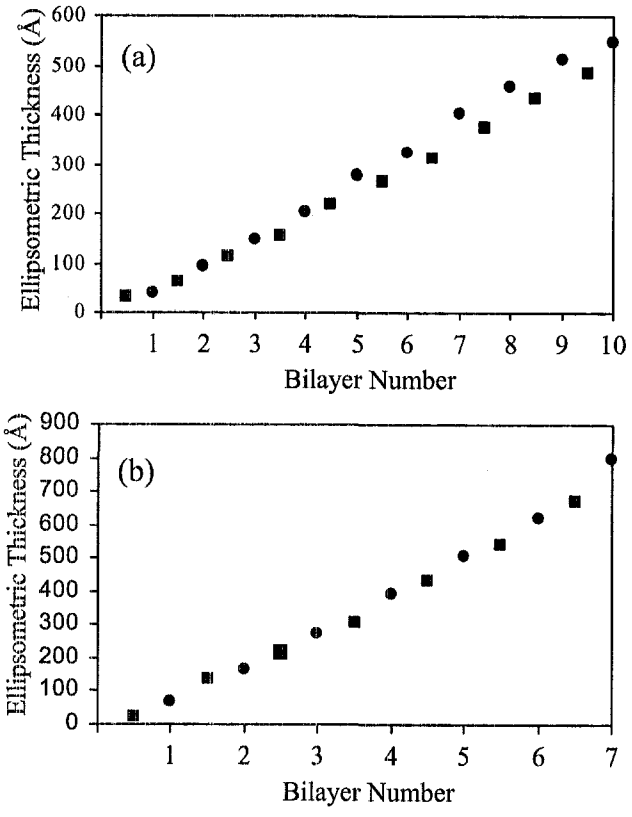
(a)
Ellipsometric Thickness (Å)
0
100
200
300
400
500
600
1
2
3
4
5
6
7
8
9
10
Bilayer Number
(b)
Ellipsometric Thickness (Å)
0
100
200
300
400
500
600
700
800
900
1
2
3
4
5
6
7
Bilayer Number

Figure 6

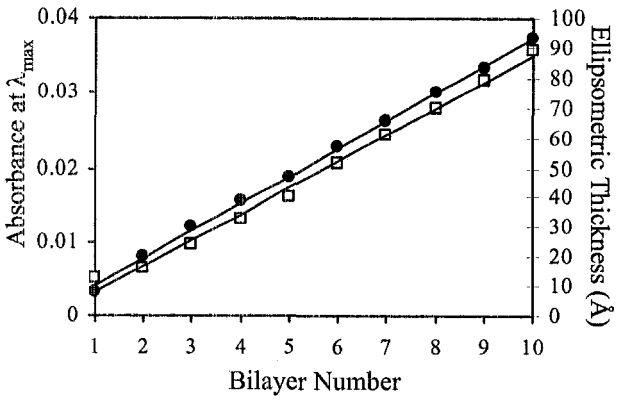
Absorbance at λ_{max}
0.04
0.03
0.02
0.01
0
Ellipsometric Thickness (Å)
100
90
80
70
60
50
40
30
20
10
0
1
2
3
4
5
6
7
8
9
10
Bilayer Number

Figure 7

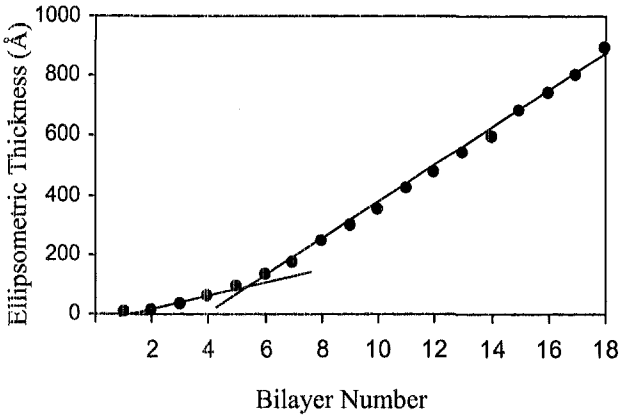
Ellipsometric Thickness (Å)
1000
800
600
400
200
0
2
4
6
8
10
12
14
16
18
Bilayer Number

Figure 8

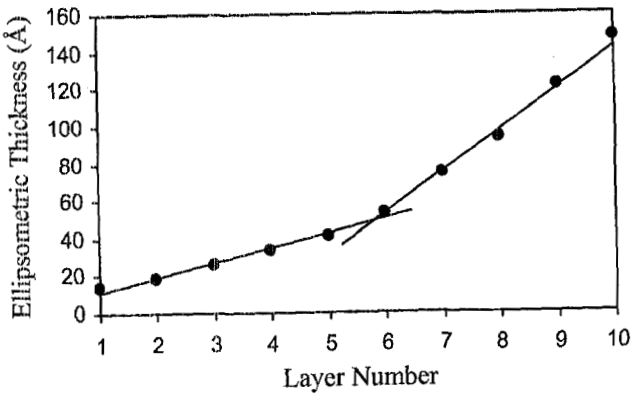
Ellipsometric Thickness (Å)
160
140
120
100
80
60
40
20
0
1
2
3
4
5
6
7
8
9
10
Layer Number

Figure 9.

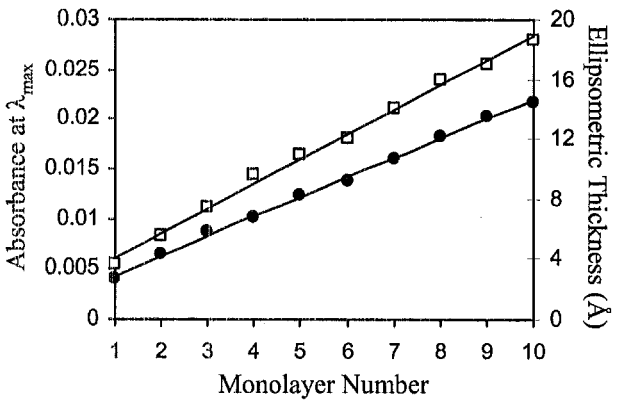

Monolayer Number